Edinburgh Research Explorer

Exploiting Supramolecular Interactions to Control Isomer Distributions in Reduced-Symmetry [Pd2L4]4+ Cages

Link:
Link to publication record in Edinburgh Research Explorer

Document Version:
Peer reviewed version

Published In:
Inorganic Chemistry

Exploiting Supramolecular Interactions to Control Isomer Distributions in Reduced-Symmetry [Pd$_2$L$_4$]$^{4+}$ Cages

Roan A. S. Vasdev,[a,b] Dan Preston, [a,b]† Caitlin A. Casey-Stevens, [a,b] Vicente Martí-Centelles, [c]†

Paul J. Lusby, [c] Anna L. Garden, [a,b] and James D. Crowley [a,b] ∗

AUTHOR ADDRESS

[a]Department of Chemistry, University of Otago, PO Box 56, Dunedin 9054, New Zealand

Email: jcrowley@chemistry.otago.ac.nz

[b]MacDiarmid Institute for Advanced Materials and Nanotechnology, New Zealand

[c]EaStCHEM School of Chemistry, Joseph Black Building, David Brewster Road, Edinburgh EH9 3FJ, Scotland

ABSTRACT

High symmetry metallosupramolecular architectures (MSAs) have been exploited for a range of applications including molecular recognition, catalysis and drug delivery. Recently there have been increasing efforts to enhance those applications by generating reduced symmetry MSAs. Here we report our efforts to use supramolecular (dispersion and hydrogen bonding) forces and solvophobic effects to generate isomerically pure $[Pd_2(L)_4]^{4+}$ cage architectures from a family of new reduced symmetry ditopic tripyridyl ligands. The reduced symmetry tripyridyl ligands featured either solvophilic polyether chains, solvophobic alkyl chains or amino substituents. We show using NMR, HPLC, X-ray diffraction data and DFT calculations that a combination of dispersion forces and solvophobic effects does not provide any control of the $[Pd_2(L)_4]^{4+}$ cage isomer distribution with mixtures of all four cage isomers (HHHH, HHHT, *cis*-HHTT or *trans*-HTHT, H = head and T = tail) obtained in each case. More control was obtained by exploiting hydrogen bonding interactions between amino units. While cage assembly with a 3-amino-substituted tripyridyl ligand lead to a mixture of all four possible isomers, the related 2-amino-substituted tripyridyl ligand generated a *cis*-HHTT cage architecture. The formation of the *cis*-HHTT $[Pd_2(L)_4]^{4+}$ cage was confirmed using NMR studies and X-ray crystallography.

Introduction

Self-assembled coordination complexes, and in particular metallosupramolecular architectures (MSAs), have been subject to increasing interest[1-8] due to their many potential applications. The molecular recognition properties of these systems have been exploited to encapsulate environmental pollutants[9-10] and reactive species.[11-13] These systems have also been used for catalysis[14-18] and as drug delivery vectors.[19-22] Additionally, MSAs have been utilized as molecular

flasks,[23-26] and their biological,[27-29] electronic,[30-32] redox[33-34] and photophysical[35-37] properties have been extensively examined.

Nature has been developing self-assembled and noncovalent folded molecules for specific purposes, such as catalysis, for millennia. Most biological systems are typically (but not always[38-40]) characterized by low symmetry as these can be much more effective as they are tailored to recognize the vast majority of substrates, intermediates and transition states that possess little or no symmetry elements. In contrast, virtually all the accomplishments that have been achieved with MSAs have utilized high-symmetry structures; these are significantly easier to prepare due to the limitations of thermodynamic assembly reactions, where reversibility leads to multiple species of similar energy, maximizing global entropy. As such, wholly synthetic, reduced-symmetry MSAs are not only more desirable as functional systems, they also push the boundaries of current self-assembly methods.[41-44]

While almost any metal ion with a correctly designed ligand system can be exploited to generate MSAs, palladium(II) based architectures[45-46] represent one of the largest subsets of these materials. In particular, $[Pd_2(L)_4]^{4+}$ cage architectures, first reported by McMorran and Steel,[47] have been extensively studied.[45-46, 48-52] Their molecular recognition properties with neutral organic[12, 53-60], inorganic[61-65] guests and anions[66-75] have been extensively examined. They have also been exploited for drug delivery[76] and catalysis.[77-80] Additionally, $[Pd_2(L)_4]^{4+}$ cage architectures have been at the forefront of efforts to develop reduced symmetry MSAs (Figure 1).[81-84] This is presumably because they are assembled from relatively few components (six: four ligands and two metal ions) and the synthesis of the diheterocyclic ligands used to assemble the cages is usually facile. Several different groups have developed methods for the generation of lower symmetry $[Pd_2(L)_4]^{4+}$ cage architectures that feature different ligands. $[Pd_2(L_x)_2(L_y)_2]^{4+}$ cages, both cis[85-86]

and trans[87] isomers, and $[Pd_2(L_a)_3(L_b)]^{4+}$ cage systems[88] (Figure 1) have been generated by exploiting geometric complementarity or steric control.[89] These approaches have been further extended to develop larger heteroleptic $[Pd_n(L_x)_n(L_y)_n]^{2n+}$ cage architectures (where n = 4, 6 and 8),[42, 90] and very recently a heteroleptic $[Pd_3(L_x)_2(L_y)_3]^{6+}$ cage has been generated by elegantly exploiting geometric complementarity.[91] Guest templates (C_{60}) have also been used to bias the formation of a heteroleptic cis-$[(C_{60})\subset Pd_2(L_c)_2(L_d)_2]^{4+}$ cage−guest adduct.[92]
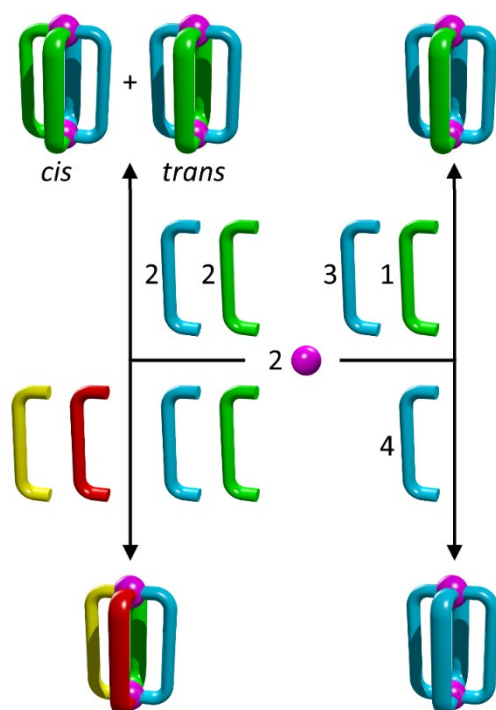
Figure 1: Cartoons depicting the different types of hetero and homoleptic $[Pd_2(L)_4]^{4+}$ cages. Cis- and trans-$[Pd_2(L_A)_2(L_B)_2]^{4+}$ (top left) and $[Pd_2(L_A)_3(L_B)]^{4+}$ (top right). A hypothetical tetra-heteroleptic $[Pd_2(L_A)(L_B)(L_C)(L_D)]^{4+}$ cage (bottom left) and the more common homoleptic $[Pd_2(L)_4]^{4+}$ cage (bottom right).

We have also synthesized a *cis*-$[Pd_2(tripy)_2(2A\text{-}tripy)_2]^{4+}$ cage, by using unsubstituted (tripy = 2,6-bis(pyridin-3-ylethynyl)pyridine) and 2-amino-substituted tripyridyl ligands (2A-tripy = 5,5'-(pyridine-2,6-diylbis(ethyne-2,1-diyl))bis(pyridin-2-amine), Figure 2).[93] The formation of the *cis-*

heteroleptic system was achieved through hydrogen bonding and steric effects.[86, 94] Interestingly, density function theory (DFT) calculations indicated that the *cis*-[Pd$_2$(tripy)$_2$(2A-tripy)$_2$]$^{4+}$ system was a long lived kinetically metastable intermediate rather than the thermodynamic product of the reaction. While these systems, along with others,[88, 92] have been desymmetrized in one dimension, giving mixed ligand architectures, the two palladium ions are in the same environment. An alternative approach to low/reduced symmetry [Pd$_2$(L)$_4$]$^{4+}$ cage architectures would be to use lower symmetry ligands where the two "ends" are different. This would lead to four potential isomeric outcomes; a head-to-head-to-head-to-head (HHHH), a head-to-head-to-head-to-tail (HHHT), a cis-head-to-head-to-tail-to-tail (cis-HHTT) or trans-head-to-tail-to-head-to-tail (trans-HTHT) [Pd$_2$(L)$_4$]$^{4+}$ cage systems (Figure 2). Efforts to generate these types of low symmetry [Pd$_2$(L)$_4$]$^{4+}$ cages isomerically pure have been developed recently.[95] Lewis and co-workers[96-97] (and others[98]) have used both steric effects and geometric complementarity in dipyridyl ligands to generate isomerically pure [Pd$_2$(L)$_4$]$^{4+}$ cage systems with lateral asymmetry.[96-97] This has been extended to [Pd$_n$(L)$_{2n}$]$^{4+}$ cages (where n = 4 or 6) as well.[99] In an alternative approach the Yuasa,[100] Chand[101] and Lewis[102] groups have used low-symmetry ligands that feature one pyridyl donor site and a second different donor unit (either an imidazole, a 1,2,3-triazole or an aryl amine) to selectively from the cis-HHTT [Pd$_2$(L)$_4$]$^{4+}$ cage isomers. There is only one reported attempt to use non-covalent/supramolecular forces to generate low symmetry [Pd$_2$(L)$_4$]$^{4+}$ cages isomerically pure. Natarajan and co-workers have exploited hydrogen bonding interactions between alcohol functionalised low symmetry dipyridyl amide ligand based on cholic acid (L$_{cholic}$). DFT calculations indicated that the HHHH [Pd$_2$(L$_{cholic}$)$_4$]$^{4+}$ isomer was the most stable.[103] However, ^{1}H NMR spectra of the cage mixtures were broad (even at 343 K) and do not provide clear insight into the isomer distribution within the system and no crystallographic evidence was obtained.

Additionally, hydrogen bonding interactions in amide[104-105] and urea[106] functionalized $[Pd_2(L)_4]^{4+}$ cages have been used to generate lower symmetry cage conformations in the solid state.

Building on our other work with $[Pd_2(L)_4]^{4+}$ cage architectures,[61-63, 66, 70-71, 107-108] we targeted the formation of isomerically pure $[Pd_2(L)_4]^{4+}$ cage architectures, where the two palladium(II) ions are in different environments, using low-symmetry ligands and solvated palladium(II) ions. We proposed to achieve this through the use of supramolecular (dispersion and hydrogen bonding) forces and solvophobic effects.[109-110] We have generated a family of new low symmetry tripyridyl ligands featuring hydrophilic polyether chains, hydrophobic alkyl chains or amino substituents (Figure 2). For ligands featuring the hydrophobic alkyl chains the combination of solvophobic and dispersion forces could potentially lead to aggregation/clumping of those groups influencing the isomer distribution, as has been observed by others in macrocyclic systems.[109-110] Alternatively, for the ligands appended with the amino units a combination of steric effects and hydrogen bonding could affect the isomer distributions of the cage.[88, 92] In both cases the overall symmetry of the cages is reduced/lowered relative to the parent $[Pd_2(L)_4]^{4+}$ system. However, the micro/local symmetry of the cage cavity is unaffected. Herein we describe the synthesis of a series of new $[Pd_2(L)_4]^{4+}$ cage architectures from these low symmetry tripyridyl ligands along with observed isomer distributions of the cages. It is shown that certain supramolecular forces are more useful than others in providing control over the isomer distributions.

Results and Discussion

Ligand synthesis

To test if dispersion forces and solvophobic effects could produce a uniform single cage isomer, ligands with both polyether and alkyl chains (**L1**, **L2** and **L3**), only polyether chains (**L4**, **L6** and

L8) or only alkyl chains (**L5**, **L7** and **L9**) were synthesized. Additionally, we have previously used the hydrogen bonding effect between amino-functionalized ligands to generate cis-$[Pd_2(tripy)_2(2A\text{-}tripy)_2]^{4+}$ heteroleptic cages, thus low-symmetry amino-substituted ligands (**L10** and **L11**) were also synthesized to assess whether a single isomer cage could be formed by using hydrogen bonding as the main driving force.

Exploiting methods reported previously by ourselves[61-63, 66, 70-71, 107-108] and others[53, 80, 88, 111-112] we synthesised a family of new low symmetry tripyridyl ligands using the standard procedures outlined in the Supporting Information (**L1** – **L11**, 60-75%, Figure 2, Supporting Information). There are four distinct sub families of ligands, **L1-L3** feature an alkyl chain at one end and a polyether chain at the other, with the length of the chains decreasing across the series. **L4**, **L6** and **L8** are singly substituted with ethylene glycol chains of different length, featuring either one (**L8** monoethylene glycol (MEG)), two (**L6** diethylene glycol (DEG)) or four (**L4** tetraethylene glycol (TEG)) repeat units.

L5, **L7** and **L9** are singly substituted with a linear alkyl chain (again of differing chain lengths, **L5** = dodecyloxy (DdO), **L7** = hexyloxy (HexO), **L9** = propyloxy (PrO). Additionally, two ligands featuring an amine substituent at one end (**L10**, 2-amino, **L11** 3-amino) were generated (Figure 2 and Supporting Information). Each new low-symmetry ligand was characterized through ^1H and ^{13}C NMR spectroscopies, mass spectrometry and elemental analysis. For example, ^1H NMR spectroscopy of **L1** in CD_3CN (Supporting Information) revealed nine distinct peaks in the aromatic region, as well as signals arising from TEG and DdO chains. A diffusion-ordered spectroscopy (DOSY) NMR spectrum of the ligand showed that all proton resonances displayed the same diffusion coefficient (D = 3.61×10^{-10} m^{-2} s^{-1}, Supporting Information). High-resolution electrospray mass spectrometry (HR-ESMS) showed a single isotopically resolved peak at

694.3839 m/z (calc. m/z = 694.3827 [**L1**+Na]$^+$), which was assigned to the sodiated ligand, providing further evidence for the generation of the ligand. ^{13}C NMR spectroscopy, along with elemental analysis was consistent with the clean formation of **L1** (Supporting Information). Ligands **L2** – **L11** displayed similar spectral properties (Supporting Information).
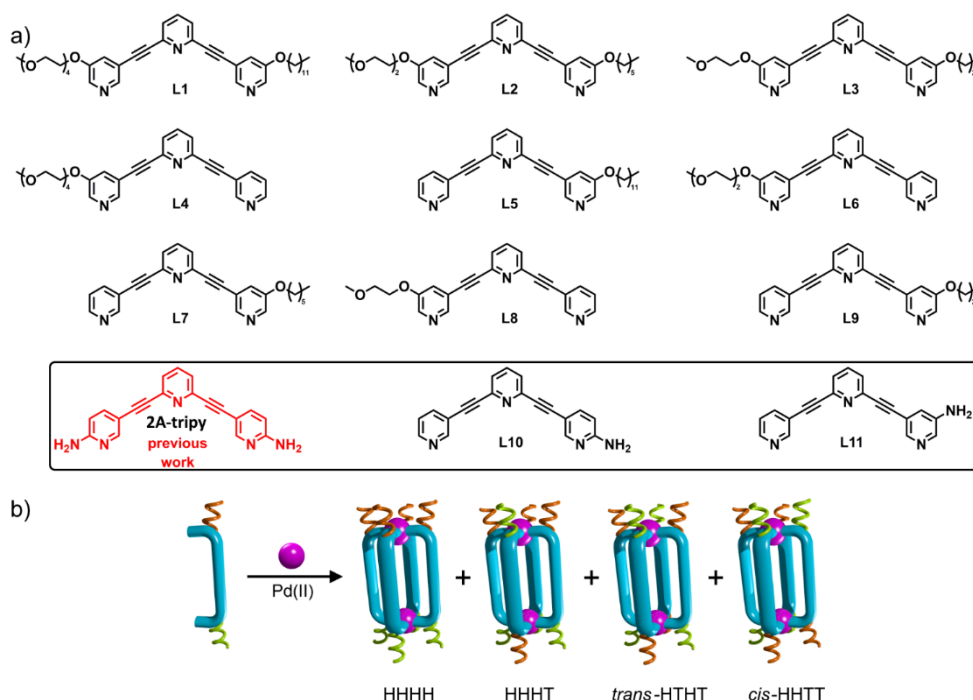
Figure 2: a) The family of low-symmetry tripyridyl ligands (**L1-L11**) and **2A-tripy**.[93] b) Cartoon representation of the HHHH, HHHT, *trans*-HTHT and *cis*-HHTT isomers of the [Pd$_2$(L)$_4$]$^{4+}$ cage architectures. H = head and T = tail

Cage synthesis with L1-L9

The cages **C1-C9** were synthesized by reacting each low-symmetry ligand (**L1-L9**) in a 4:2 ratio with Pd(NO$_3$)$_2$·2H$_2$O in dimethylformamide (DMF) at 40 °C for 14 hours. Precipitation with a 1:4 mixture of diethyl ether and petroleum ether (40-60) resulted in colorless-tan solids that were collected through centrifugation or filtration. In situ ^{1}H NMR spectra indicated that the cages

formed quantitatively as no signals due to the "free" ligands were observed. However, due to their solubility, the cages were only isolated in 65-76% yield. Electrospray ionization mass spectral analysis of each of the cages (**C1-C9**) showed a series of peaks consistent with the formation of the $[Pd_2(L)_4]^{4+}$ cage; every spectrum displayed ions due to $[Pd_2(L)_4]^{4+}$ and $[Pd_2(L)_4](X^-)^{3+}$ (where $X = NO_3^-$, Cl^-, or HCO_2^-) with some spectra also displaying ions due to $[Pd_2(L)_4](2X^-)^{2+}$ and fragmentation (Supporting Information). The ^1H and ^1H DOSY NMR spectroscopic data of the cages (**C1-C9**) were also consistent with cage formation. For each of the cages (**C1-C9**) the proton resonances due to the terminal pyridine unit were shifted downfield (0.5-1.0 ppm) relative to the "free" ligands, consistent with coordination to the cationic Pd(II) ions (Supporting Information), and similar to what has been observed for related $[Pd_2(L)_4]^{4+}$ cages. ^1H DOSY NMR data were obtained for each cage and showed that each cage was diffusing at a slower rate than its corresponding ligand, providing further evidence for the generation of the cages. Additionally, the observed diffusion coefficients (Supporting Information), were similar to those found for related $[Pd_2(L)_4]^{4+}$ cages.[53, 61-62, 66, 70-71, 80, 88, 107-108, 111-113]

Closer inspection of the ^1H NMR spectra (400 MHz, d_7-DMF) of **C1-C3** showed relatively sharp spectra displaying what appeared to be a single set of resonances consistent with the formation of a single isomer (Supporting Information). Disappointingly, despite the presence of the ethylene glycol substituents and nitrate counter anions the cages were not soluble in water/D_2O. However, **C1-C3** did display excellent solubility in a range of polar solvents and we were able to obtain ^1H NMR spectra in d_7-DMF, d_6-DMSO, CD_3CN, CD_3NO_2, CD_3OD and d_6-acetone (Supporting information). Like the d_7-DMF spectra the data obtained were sharp and for the most part seemed consistent with the presence of a single isomer. In contrast to the data obtained for the **C1-C3** cages, the ^1H NMR spectra (400 MHz, d_7-DMF) of the cages with glycol chains (**C4, C6** and **C8**)

and alkyl groups (**C5**, **C7** and **C9**) indicated that mixtures of isomers were obtained as there were multiple resonances observed for each different proton (Supporting Information). Unfortunately, determining the exact isomer ratio for the **C4-C9** cages using the ^{1}H NMR data proved impossible due to peak overlap. However, ^{1}H NOESY NMR spectra (500 MHz) provided additional support for the presence of isomers (Supporting Information). The ortho pyridyl protons (H_a, H_d, H_h and H_i) could be identified and NOE through-space coupling between H_d and H_h was observed. This was consistent with the presence of the HHHT, and *trans*-HTHT and *cis*-HHTT isomers in solution (Figure 3 and Supporting Information).

High Performance Liquid Chromatography[114] (HPLC, C-18 column, CH_3CN, 5% TFA)[93] was used to gain further insight into the isomeric mixtures for the cages (**C1-C9**) (Figure 3 and Supporting Information). The glycol containing **C4**, **C6**, **C8** cages all had similar retention times (~ 8 minutes) with the **C4**, **C6** and **C8** cage mixtures displaying three peaks (two smaller peaks flanking a larger broad peak). These results suggest cage mixtures contain at least three of the four expected cage isomers, although the broad nature of the larger central peak may indicate that it is in fact two overlapping peaks.

The **C5**, **C7** and **C9** cage mixtures (the cages featuring the alkyl chains) all have different retention times (**C5** ~ 15 mins, **C7** ~ 12 mins and **C9** ~ 9 mins) due the longer alkyl chains interacting more strongly with the C18 column and they all clearly displayed four peaks, one for each of the expected cage isomers suggesting that we obtain a mixture that features all the possible cage isomers (Figure 3 and Supporting Information).

The HPLC data showed that **C1-C3** cages were also mixtures of all four of the possible cage isomers, similar to what was observed for the **C4-C9** cages. The retention times for the **C1-C3**

cages tracked the alkyl chain length similar to the **C5**, **C7** and **C9** systems. The **C1** (retention time ~ 15 minutes) and **C2** (retention time ~ 12 minutes) cages clearly displayed four peaks due the isomers, while the **C3** cage (retention time ~ 10 minutes) with the shortest substituents showed three peaks, a larger very broad peak flanked by two smaller peaks (Figure 3, Supporting Information).
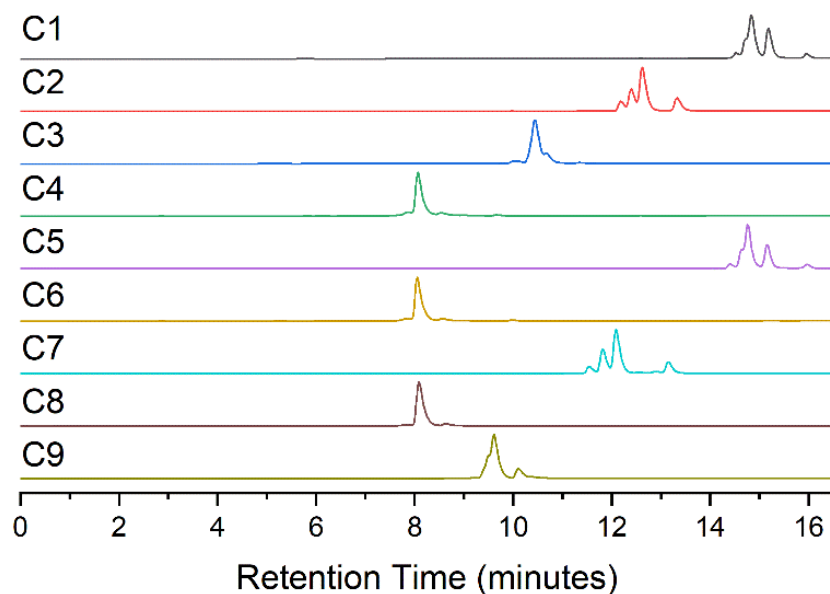

Figure 3: HPLC traces (C-18 column, CH_3CN, 5% TFA) for the cages **C1-C9**.

To supplement the experimental data, density functional theory (DFT) calculations were undertaken using the BP86 functional with the def2-SVP basis set and a DMF solvent field (Supporting Information).[115] Consistent with the experimental results, the calculations showed that there are only small differences in the energies of the different cages isomers (**C1-C9**). For the alkyl substituted cages (**C5**, **C7** and **C9**) the calculations showed that the lowest energy isomer, in each case, was the HHHH system. The calculated energies of the four cage isomers only differed by a maximum of 3.23 kJ/mol, consistent with the experimental observation of mixtures. Interestingly, the calculations of the alkyl substituted cages (**C4**, **C6** and **C8**) indicated that the

trans-HTHT isomer was the most stable for each of the three different substituted cages. Once again, however, the energy difference between the all isomers are small (<5 kJ/mol, Supporting Information).

The calculations for **C1-C3** indicated that in each case the HHHH isomer was the lowest energy species. However, the energy differences between the most stable and least stable isomers were small (5.14 kJ/mol for **C1**, 3.11 kJ/mol for **C2** and 4.59 kJ/mol for **C3**) (Figure 4 and Supporting Information). These calculated energy differences for **C1-C3** were similar to those observed for the **C4-C9** cages. Thus, the DFT result are consistent with the HPLC data and indicate that all the cages (**C1-C9**) exist as mixture isomers.
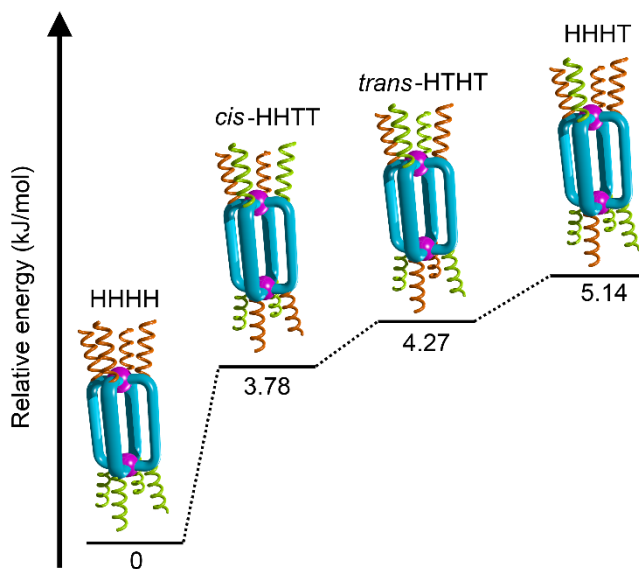
Figure 4: Energy diagram showing the energy difference between the different cage isomer of the $[Pd_2(\textbf{L1})_4]^{4+}$ cage (**C1**) obtained from DFT calculations.

The DFT calculations and HPLC data strongly suggest that the **C1-C3** cages exist as mixture of all cage isomers. This, however, was inconsistent with the NMR data obtained at 400 MHz (*vide supra*, and Supporting Information). We postulated that the isomers of the **C1-C3** cages have

coincident/overlapping resonances at 400 MHz, this possibly due very similar electronic environments of the two "ends" of the ligands. Therefore, we obtained the ^{1}H NMR spectra (d_7-DMF) of **C1-C3** at 800 MHz (Figure 5 and Supporting Information). At the higher field strength, it was immediately apparent that the cages were mixtures, there were clearly multiple different resonances due to the exo protons H_a and H_i of the terminal pyridyl units consistent with the presence of more than one cage isomer. Unfortunately, due to signal overlap we were unable to use the NMR data to gain insight in the isomer ratios.

Additionally, ^{1}H NOESY 2D NMR spectra obtained at 800 MHz was employed to probe the existence of isomers further. Several cross-peaks between the ortho pyridyl protons on the terminal pyridine units of opposing ligands, i.e. cross-peaks between H_a and H_i, and H_c and H_g were observed. The NOESY spectra also displayed some cross-peaks, from the H_j and H_o protons (the first CH_2 units of the alkyl and polyether substituents, (Figure 5c and Supporting Information). These cross peaks are consistent with the presence of HHTT, HTHT, and HHHT isomers within the mixture. Overall the collected data suggest that mixtures of isomers are obtained for all the generated cages **C1-C9**.
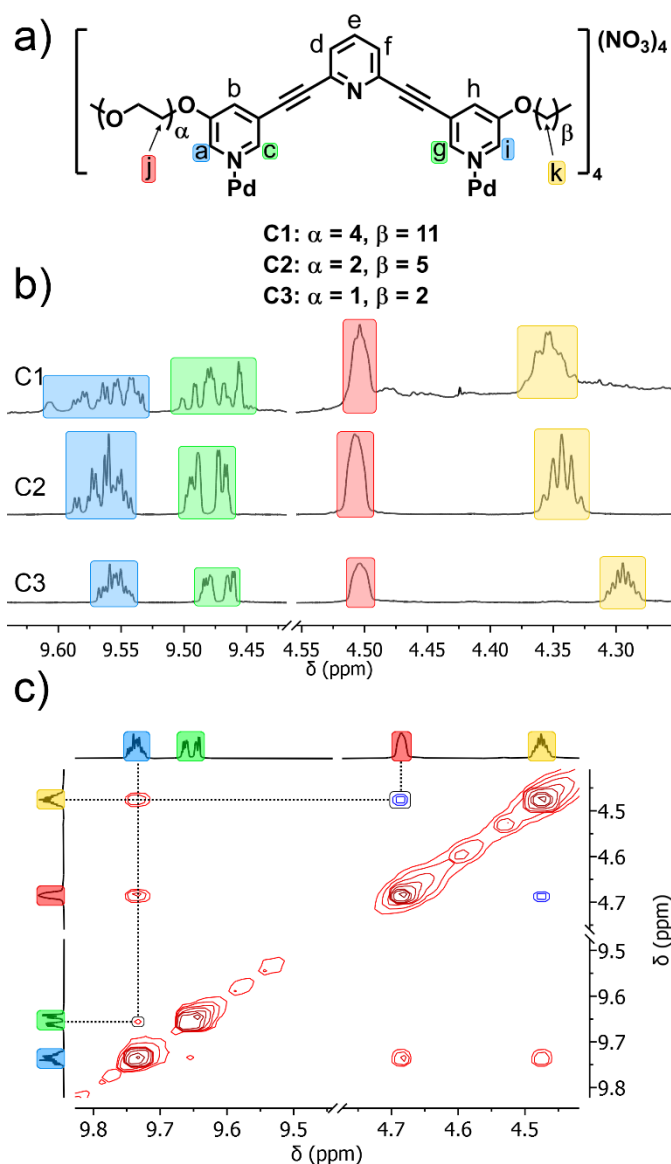
Figure 5: a) Labelled chemical structure of **C1-C3**; b) partial stacked ^{1}H NMR spectrum (800 MHz, d$_7$-DMF, 298 K) of **C1**, **C2** and **C3** showing signals from ortho pyridyl protons H$_a$, H$_c$, H$_g$ and H$_i$ overlapping; and c) partial ^{1}H NOESY spectrum (800 MHz, d$_7$-DMF, 298 K) of **C3** with cross-peaks between H$_{a,i}$ and H$_{c,g}$, and H$_j$ and H$_m$.

Remarkably, further evidence for the presence of isomeric mixtures was obtained using X-ray crystallography (Figure 6 and Supporting Information). Rhombic, yellow crystals of the **C9** cage (propyloxy (OPr) substituted) suitable for X-ray diffraction were obtained via vapor diffusion of

14

diethyl ether into a DMF solution of the cage mixture. The structure was solved in the triclinic space group $P\bar{1}$, with the asymmetric unit containing two ligands, one palladium(II), a DMF molecule and a nitrate counterion. While the structure was disordered, and could potentially be modelled in a range of ways all the sensible solutions were consistent with the presence of a mixture of cage isomers. We found that freely refining the data from the **C9** cage as mixture of the HHHH, HHHT, *trans*-HTHT and the *cis*-HHTT isomers (Figure 6, Supporting Information) provided a reasonable solution with the observed ratios of the four isomers similar to what was expected from statistics (Supporting information). The Pd-N bond lengths (2.025-2.038 Å) and the Pd-Pd distance (11.836 Å) are similar to those observed in related $[Pd_2(L)_4]^{4+}$ cages,[53, 61-62, 66, 70-71, 80, 88, 107-108, 111-113] and two DMF guest molecules occupy the cavity of the cages (Figure 5 and Supporting Information).
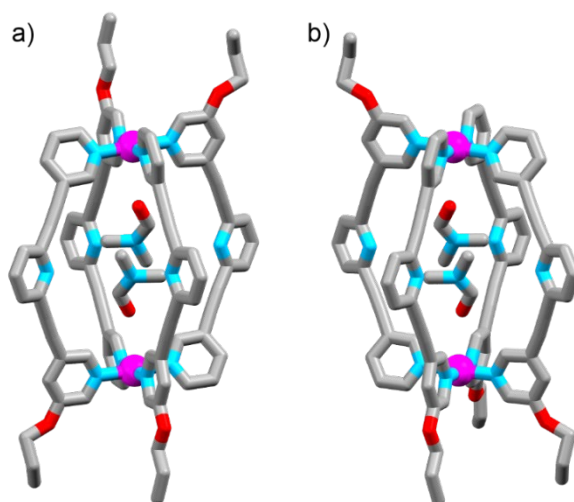

Figure 6: Tube representations showing the two major isomers of the $[Pd_2(\textbf{L9})_4]^{4+}$ cage (**C9**) observed via X-ray crystallography: a) cis-HHTT cage isomer and b) HHHT isomer. Colours: Grey = carbon, red = oxygen, blue = nitrogen and magenta = palladium. Counter-anions omitted for clarity.

Cage synthesis with the amino substituted ligands L10-L11

Having established that that dispersion/solvophobic effects were not sufficient to provide isomerically pure low symmetry cages, we next investigated our second targeted supramolecular interaction, hydrogen bonding. We have previously used 2-amino substituted tripyridyl ligands to generate a heteroleptic cis-[Pd$_2$(tripy)$_2$(2A-tripy)$_2$]$^{4+}$ cage by exploiting hydrogen bonding and steric effects afforded by the 2-amino group.[93] We targeted the same approach here in order to generate an isomerically pure low symmetry [Pd$_2$(L)$_4$]$^{4+}$ cage. The 2-amino substituted ligand (**L10**) and the isomeric 3-amino substituted ligand (**L11**) could be complexed to Pd(II) ions in two different ways. The ligands (either **L10** or **L11**) were added to Pd(NO$_3$)$_2$·2H$_2$O in a 4:2 stoichiometric ratio and heated at 50 °C for 14-72 hours in DMF (Supporting Information). The cages (**C10** and **C11**) could be isolated from the reaction mixtures as tan solids upon the addition of diethyl ether. Alternatively, the cages (**C10** and **C11**) could be generated by heating (50 °C) a mixture of one of the ligands (**L10** or **L11**, 4 equiv.) with [Pd(CH$_3$CN)$_4$](BF$_4$)$_2$ (2 equiv.) for 24-72 hours (Supporting Information). In both methods the more hindered **C10** cage was formed more slowly than the **C11** system. ESI-MS data on the cages indicated that [Pd$_2$(L)$_4$]$^{4+}$ architectures were obtained (Supporting Information). ^{1}H NMR spectra of **C10** and **C11** suggested, consistent with expectations, that the **C10** cage was isomerically pure while **C11** was a mixture of isomers.[116] The ^{1}H NMR spectrum (d$_7$-DMF) for **C11** exhibited an untidy aromatic region with overlap peaks consistent with an isomeric mixture while the ^{1}H NMR spectrum for cage **C10** was pleasingly different, displaying a single set of peaks, downfield shifted when compared to the free ligand **L10**, presumably due to the formation of a single cage isomer (Figure 7 and Supporting Information). A very large downfield shift, relative to free **L10**, was observed for the proton

resonances of the 2-amino unit ($\Delta\delta$ = 2.04 ppm, d_6-DMSO) suggestive of a strong intramolecular hydrogen bonding interaction (Figure 7 and Supporting Information).[93, 108]

The ^{1}H ROESY NMR spectrum (d_6-DMSO) of **C10**, displayed cross-peaks between the endohedral pyridyl protons, H_c and H_g. Additionally, there was a through-space coupling between the 2-amino protons and H_j. The ^{1}H NMR and ROESY data was consistent with the formation of either cis-HHTT or trans-HTHT isomer (Supporting Information). However, given that the related cis-[Pd$_2$(tripy)$_2$(2A-tripy)$_2$]$^{4+}$ heteroleptic cage[93] was generated from a 2-amino substituted ligand, it seemed likely that **C10** would have formed the cis-HHTT isomer.
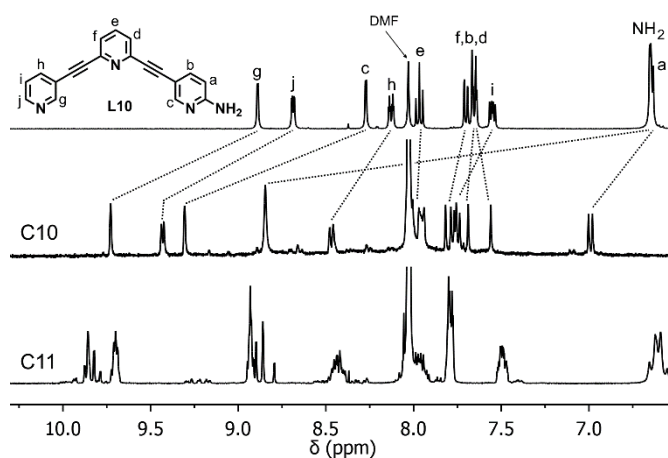
Figure 7: Partial stacked ^{1}H NMR spectra (400 MHz, d_7-DMF, 298 K) of **L10**, **C10** and **C11**.

This was confirmed using X-ray crystallography (Figure 8 and Supporting Information). Yellow, cubic, X-ray quality crystals were grown via vapor diffusion of diethyl ether into a solution of DMSO/acetonitrile of the **C10** cage. While there was some disorder present, the structure was solved in the primitive triclinic space group P$\overline{1}$, with the asymmetric unit comprising four half-cages (two ligands and one palladium(II) ion) and four DMSO solvent molecules. Each of the four

crystallographically independent cages in the unit cell is generated through inversion of a half-cage. The disorder present was partial occupancy of amino groups in two of the half cages, but importantly, in the other two half-cages (and thus in their full cages), there was no partial occupancy. In these, the cage was unambiguously the cis-HHTT isomer. Given the presence of a single isomer in solution (from NMR spectroscopies), this strongly suggests that the half-cages with partial amino occupancy are also the cis isomer. The other parameters of the cage were very similar to related $[Pd_2(L)_4]^{4+}$ systems,[53, 61-62, 66, 70-71, 80, 88, 107-108, 111-113] the Pd-Pd distances ranged from 12.302-12.718 Å. The Pd-N_{py} (range from 2.019-2.100 Å) and Pd-$N_{2aminopy}$ (range from 2.002-2.100 Å) bond distance were very similar. The cavity of the $[Pd_2(\mathbf{L10})_4]^{4+}$ cage contained two molecules of DMSO, these were held in place by hydrogen bonding interaction between the S=O and the acidic endo α-pyridyl protons of the host, C-H···O=S distances ranged from 3.206 - 3.299 Å, the H···O=S distances ranged from 2.311 - 2.390 Å (Figure 8 and Supporting Information). There were no obvious hydrogen bonding interactions with near linear N-H---N bond angles between the adjacent NH_2 units. This is presumably because of crystal packing effects between the cage within the extended crystal structure. The cages are tightly packed together in the unit cell with π-π interactions between the ligand backbones of adjacent cages. These interactions lead to a lantern shaped conformation (Figure 8 and Supporting information) of the $\mathbf{C10}$ metallo-cage preventing the subtle bond rotations that would allow the formation of the NH_2---H-NH hydrogen bonding interactions observed in related X-ray structures[108] and found in DFT calculations (vide infra). The N---N distances between the 2-amino units in the different cages are within the range (3.352-3.496 Å) observed for weak hydrogen bonding[117] and for the most part the observed distances are shorter than what was found in a related $[Pd_2(L)_4]^{4+}$ that also featured intra-molecular hydrogen bonding between amino units.[108] This suggests that once dissolved in solution

the expected *intra*-molecular hydrogen bonds could readily form via a small bond rotation. Additionally, NCIPlot analysis[118] of the crystal data was used to show that there are non-covalent interaction between the NH_2 units (Supporting Information). So, while the crystallographic data confirms the formation of the cis-HHTT isomer of **C10** it does not offer strong evidence for the expected intra-molecular hydrogen bonding between the adjacent amino units. Therefore DFT calculations (BP86 functional, def2-SVP basis set applied to all atoms except the amine groups, these were subject to the ma-def2-SVP basis set which is larger and includes diffuse functions to account for longer range interactions, DMSO solvent field, Supporting Information) were carried out on the cis-HHTT **C10** and the other three isomers (Figure 9 and the Supporting Information).[115] The DFT calculation for the cis-HHTT isomer of **C10** clearly displays an *intra*-molecular hydrogen bonding interaction (N---N distance 3.17 Å N-H---N distance 2.17 Å and N-H---N angle 164.55°) between the cis-NH_2 units as has been observed both crystallographic and computationally in related cage systems. [93, 108] This *intra*-molecular hydrogen bonding interaction is consistent with the large change in the chemical shift ($\Delta\delta$ = 2.04 ppm, d_6-DMSO) of the amino units observed in the ^{1}H NMR data of the **C10** complex relative to **L10**. However, we cannot completely rule out an *inter*-molecular bifurcated hydrogen bonding interaction between the adjacent NH_2 unit and either solvent (DMF or DMSO) or counter anions (NO_3^- or BF_4^-). Indeed, it may be that both types hydrogen bonding interaction are present and help lead to the cis-HHTT isomer of **C10.** Having said that, the *inter*-molecular bifurcated hydrogen bonding interaction is entropically less likely. Additionally, it would be expected that the amino units in the related **C11** system could also engage in *inter*-molecular bifurcated hydrogen bonding interactions with the solvent and counter anions. Thus, if this was an important factor in the controlling the isomer distribution some selectivity should be observed in the **C11** cage formation. However, the ^{1}H NMR

data are not consistent with that postulate (Figure 7 and Supporting Information) suggesting the *inter*-molecular bifurcated hydrogen bonding interactions are not the major driving force for the formation of the cis-HHTT isomer of **C10.**
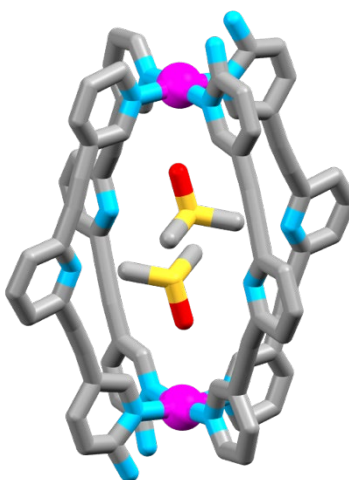

Figure 8: Tube representation of the cis-HHTT of the $[Pd_2(\mathbf{L10})_4]^{4+}$ cage (**C10**) obtained via X-ray crystallography. Colours: Grey = carbon, red = oxygen, blue = nitrogen, yellow = sulfur and magenta = palladium.
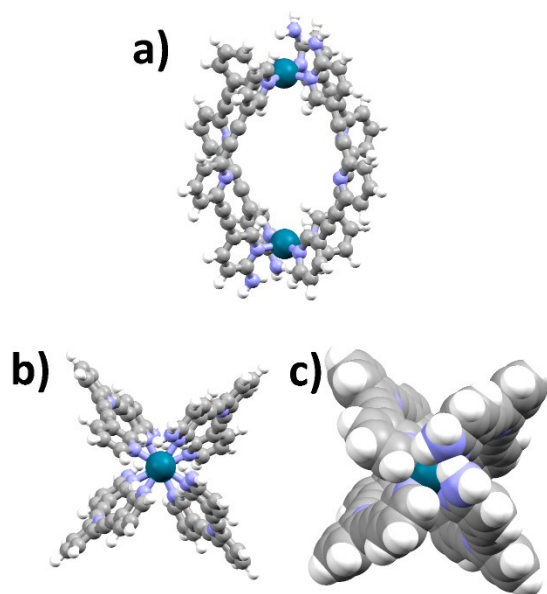
Figure 9: The calculated structure of the **C10** HHTT isomer: a) Ball-and-stick model (side view); b) Ball-and-stick model (top view); c) Space-filling model (side view). There are two hydrogen bonding interactions between the NH_2 units of the cage. The top hydrogen bonding interaction has an N···N (N···H-N) distance of 3.185 (2.194) Å, the bottom hydrogen bonding interaction has an N···N (N···H-N) distance of 3.170 (2.170) Å.

The energies of the four isomers of **C10** and **C11** were also evaluated using DFT calculations (Figure 9 and Supporting Information).[115] The energies for the four isomers of the **C11** cage were all very similar, the most stable isomer was found to be the HHHT system but there was only 2.22 kJ/mol difference between that isomer and the least stable *trans*-HTHT system (Supporting Information), consistent with the ^{1}H NMR data of **C11**. Additionally, none of the **C11** isomers displayed any *intra*-molecular hydrogen bonding interactions.

Intriguingly, the calculations on **C10** suggested that the HHHH complex had the lowest energy, with the HHHT isomer (7.77 kJ/mol higher in energy) as the second lowest energy species. The experimentally observed *cis*-HHTT isomer (8.04 kJ/mol higher in energy than the HHHH isomer)

and the *trans*-HTHT isomer was the least stable (14.19 kJ/mol higher in energy than the HHHH system, Supporting Information). Thus, the calculations confirm that the *cis*-HHTT isomer is more stable that the *trans*-HTHT isomer, but suggest that the HHHH system should be the thermodynamic product of the reaction.[119-124] This is consistent with chemical intuition, the HHHH isomer features as cyclic arrangement of four *intra*-molecular hydrogen bonds (N---N (N---H-N) distances 3.092 (2.061), 3.081 (2.050), 3.084 (2.052) and 3.090 (2.058) Å) whereas the *cis*-HHTT isomer features only two (N---N (N---H-N) distances, 3.185 (2.194) and 3.170 (2.170) Å, Supporting Information).

This is clearly not what is observed experimentally, but it was consistent with our previous results with the heteroleptic cis-$[Pd_2(tripy)_2(2A\text{-}tripy)_2]^{4+}$ cage.[93] In that case DFT calculations showed that the cis-$[Pd_2(tripy)_2(2A\text{-}tripy)_2]^{4+}$ cage was more stable than the trans-$[Pd_2(tripy)_2(2A\text{-}tripy)_2]^{4+}$ isomer, but also revealed that the homoleptic $[Pd_2(2A\text{-}tripy)_4]^{4+}$ cage was more stable than either of the heteroleptic systems, similar to what we have observed here. The isolation of the heteroleptic cis-$[Pd_2(tripy)_2(2A\text{-}tripy)_2]^{4+}$ cage instead of the energetically favored homoleptic $[Pd_2(2A\text{-}tripy)_4]^{4+}$ in that case was attributed to a combination of steric and hydrogen bonding effects which lead to a large energy barrier which prevented the formation of the homoleptic cage from the heteroleptic system. Thus, the heteroleptic cis-$[Pd_2(tripy)_2(2A\text{-}tripy)_2]^{4+}$ cage was a kinetically metastable (very) long lived intermediate rather than the thermodynamic product of the reaction. We presume, based on the DFT calculations, that similar behavior is manifest here. The experimentally observed cis-HHTT isomer of **C10** is a kinetically metastable long lived intermediate rather than the thermodynamically preferred isomer of **C10**. We have probed that postulate using ^{1}H NMR experiments (Supporting Information). The cis-HHTT isomer of **C10** was kept at 298 K in d_6-DMSO for a period of 58 days. Over that time no changes were observed

suggesting that once formed the cis-HHTT isomer is robust at RT over a period of months. Additionally, 4:2 mixtures of **L10** and either $Pd(NO_3)_2 \cdot 2H_2O$ or $[Pd(CH_3CN)_4](BF_4)_2$ were dissolved in polar solvents (either d_7-DMF or d_6-DMSO) and heated at 50 °C. The reactions were monitored using ^1H NMR spectrometry over 2-3 weeks. In each case a mixture of isomers was initially (after 6 hours) generated which more slowly converted into the cis-HHTT isomer of **C10**. In every case cis-HHTT isomer of **C10** became the dominant species in solution (>95%); for d_6-DMSO and $Pd(NO_3)_2 \cdot 2H_2O$ cis-HHTT isomer was the major species after 1 day. For the d_7-DMF solution with $Pd(NO_3)_2 \cdot 2H_2O$ and the d_7-DMF and d_6-DMSO solutions with $[Pd(CH_3CN)_4](BF_4)_2$ formation of the cis-HHTT isomer of **C10** was slower; the isomer became the dominant species (>95%) species in solution after 3-4 days. The conversion to the cis-HHTT isomer was never quantative; there was always a series of small peaks (<5%) associated with another cage isomer. This was confirmed using HPLC analysis (Supporting Information) where a large peak, due to the **C10** cis-HHTT isomer, was flanked by two very small peaks which are presumably the minor isomer observed in the NMR spectra. Continued heating (50 °C) of the d_7-DMF/**L10**/$[Pd(CH_3CN)_4](BF_4)_2$ solution led to no further changes indicating that under those conditions the cis-HHTT isomer of **C10** is robust. During prolonged heating of the d_6-DMSO/ **L10**/$[Pd(CH_3CN)_4](BF_4)_2$ solution the resonances associated with the cis-HHTT isomer of **C10** began to decrease in intensity and a new series of peaks appeared. After 15 days, the peaks from the cis-HHTT isomer have disappeared and a series of new resonances from one or more new species have grown. It was postulated that the new species could be the HHHH isomer. However, the collected ^1H NMR, ESI-MS and HPLC data show that that is not the case. The HHHH isomer should show 11 resonances in the ^1H NMR spectrum, whereas the spectrum obtained after 15 day of heating features at least 16 resonances (Supporting Information, Figure S69). The HPLC data

obtained on the mixture shows that there is no cage present only free ligand **L10** and two additional broad peaks (Supporting Information, Figure S69). ESI-MS data obtained after 16 days of heating only displayed a peak consistent with **L10**, no ions due to the **C10** cage or any other Pd(II) containing species could be identified. When combined, the NMR, HPLC and ESI-MS results indicate that, rather than forming the HHHH **C10** isomer, as the cage is heated it is slowly decomposing (similar results are obtained in other solvent *vide infra*). We postulate that the **C10** cage has lost a Pd(II) generating a mixture of isomeric Pd(II)-**L10** complexes that have different NMR spectra compared free **L10** and **C10**. Those Pd(II)-**L10** complexes then decompose further under the conditions of the HPLC and ESI-MS experiments leading to the observation of only free **L10**.

Carrying out the reaction of $[Pd(CH_3CN)_4](BF_4)_2$ and **L10** in d_6-DMSO at a higher temperature (60 and 80 °C, respectively) led to the more rapid formation of the cis-HHTT isomer but prolonged heating led to color changes from yellow to black and precipitation. Additionally, the resonances due to the cis-HHTT isomer disappeared and the NMR spectra progressively became broad and uninterpretable suggesting that the higher temperatures are simply providing more rapid access to the decomposition pathways rather than giving access to the thermodynamically preferred (from calculations) HHHH isomer. Similar results were also obtained with $Pd(NO_3)_2 \cdot 2H_2O$ in d_7-DMF and d_6-DMSO solutions. With prolonged heating (50 °C) the resonances of the cis-HHTT isomer decreased in intensity and the NMR spectra became broad and difficult to interpret. These changes are accompanied by color changes from yellow to brown/black and precipitation (Supporting Information).

Overall the collected experimental and computational results are consistent with the postulate that the cis-HHTT isomer of **C10** is a kinetically metastable (very) long lived intermediate rather than

the thermodynamic product of the reaction. However, once the cis-HHTT isomer of **C10** is formed the combination of hydrogen bonding and steric effects put in place a large energic barrier and we have not been able to isolate the HHHH isomer that was calculated to be the thermodynamic product from the reaction. All efforts to generate the HHHH isomer by heating the reaction mixture have ultimately led to cage decomposition. That behavior is similar to what was observed with the cis-$[Pd_2(tripy)_2(2A-tripy)_2]^{4+}$ cage which was also a kinetically metastable long lived intermediate rather than the thermodynamic product.[93]

Conclusions

Methods to controllably form reduced-symmetry, single isomer cages have been developed using sterics or geometric complementarity, but supramolecular interactions have not yet been extensively employed to achieve structural control. Here, we synthesized a family of reduced symmetry tripyridyl ligands (**L1-L11**) and examined if supramolecular interactions could be exploited to control the isomer distribution of the $[Pd_2(L)_4]^{4+}$ cages formed when the ligands were treated with Pd(II) ions. Inspired by the work of Stang and co-workers,[109] who had showed that dispersion forces and solvo-phobic/philic effects could be used to generate ordered metallomacrocyclic structures, we initially used a series of tripyridyl ligands (**L1-L9**) that feature either solvophobic alkyl chains, solvophilic polyether substituents or both groups. Disappointingly, NMR, HPLC data and DFT calculations showed that no control of the isomer distribution was afforded by the combination of dispersion forces and solvo-phobic/philic effects, the cages (**C1-C9**) were all mixtures of each of the four possible cages isomers (HHHH, HHHT, cis-HHTT or trans-HTHT). While dispersion forces and solvo-phobic/philic effects did not provide any control over the isomer distribution of the cages, hydrogen bonding proved more successful. We examined two further ligands systems (**L10** and **L11**) which feature 2- and 3-

aminopyridine units with the potential to engage in hydrogen bonding.[93] NMR data and DFT calculations showed the **C11** cage, assembled from the 3-aminopridine ligand **L11**, was a mixture of the four possible isomers. However, the **C10** cage (generated from the 2-aminopyridine ligand **L10**) was found to cleanly generate one single isomeric form. NMR data was consistent with the formation of either the cis-HHTT or trans-HTHT isomers of **C10**. X-ray crystallographic data confirmed that the cis-HHTT **C10** isomer was obtained. The combination of steric effects and hydrogen bonding between the amino units of the **L10** ligands drives the formation of the cis-HHTT. Lewis[96] had previously exploited steric effects and demonstrated the clean formation of a trans-HTHT $[Pd_2(L)_4]^{4+}$ cage when using a related dipyridyl ligand that featured a methyl unit in the 2 position of one of the terminal pyridyl groups. Therefore, by exploiting both steric and hydrogen bonding effects, this work provides a complementary method for the generation of the cis-HHTT cage isomer and adds to a growing range of approaches to reduced symmetry $[Pd_2(L)_4]^{4+}$ cages[102] which could in the future lead to enhanced catalytic[77-80] or molecular recognition properties.[12, 53-75]

ASSOCIATED CONTENT

Supporting Information.

The following files are available free of charge.

Experimental section, ^{1}H, ^{13}C, and DOSY NMR spectral information, HR-ESI-MS, HPLC, X-ray, and electrochemical data, DFT calculation details, and calculated structures (PDF)

DFT-calculated structures (XYZ)

AUTHOR INFORMATION

Corresponding Author

Department of Chemistry, University of Otago, P.O. Box 56, Dunedin 9054, New Zealand;

Present Addresses

Dan Preston: Research School of Chemistry Australian National University Canberra ACT 2600, Australia.

Vicente Martí-Centelles: Instituto Interuniversitario de Investigación de Reconocimiento Molecular y Desarrollo Tecnológico (IDM), Universitat Politècnica de València, Universitat de València, 46022 Valencia, Spain

Author Contributions

The manuscript was written through contributions of all authors. All authors have given approval to the final version of the manuscript.

REFERENCES

1.   Debata, N. B.; Tripathy, D.; Chand, D. K., Self-assembled coordination complexes from various palladium(II) components and bidentate or polydentate ligands. *Coord. Chem. Rev.* **2012,** *256* (17-18), 1831-1945.

2.   Smulders, M. M. J.; Riddell, I. A.; Browne, C.; Nitschke, J. R., Building on architectural principles for three-dimensional metallosupramolecular construction. *Chem. Soc. Rev.* **2013,** *42* (4), 1728-1754.

3.   Chakrabarty, R.; Mukherjee, P. S.; Stang, P. J., Supramolecular Coordination: Self-Assembly of Finite Two- and Three-Dimensional Ensembles. *Chem. Rev.* **2011,** *111* (11), 6810-6918.

4.   Beves, J. E.; Blight, B. A.; Campbell, C. J.; Leigh, D. A.; McBurney, R. T., Strategies and Tactics for the Metal-Directed Synthesis of Rotaxanes, Knots, Catenanes, and Higher Order Links. *Angew. Chem., Int. Ed.* **2011,** *50* (40), 9260-9327.

5.   Castilla, A. M.; Ramsay, W. J.; Nitschke, J. R., Stereochemistry in Subcomponent Self-Assembly. *Acc. Chem. Res.* **2014,** *47* (7), 2063-2073.

6.   Cook, T. R.; Stang, P. J., Recent Developments in the Preparation and Chemistry of Metallacycles and Metallacages via Coordination. *Chem. Rev.* **2015,** *115* (15), 7001-7045.

7.   Han, M.; Engelhard, D. M.; Clever, G. H., Self-assembled coordination cages based on banana-shaped ligands. *Chem. Soc. Rev.* **2014,** *43* (6), 1848-1860.

8.   Jansze, S. M.; Severin, K., Clathrochelate Metalloligands in Supramolecular Chemistry and Materials Science. *Acc. Chem. Res.* **2018,** *51* (9), 2139-2147.

9.   Blanco, V.; Garcia, M. D.; Terenzi, A.; Pia, E.; Fernandez-Mato, A.; Peinador, C.; Quintela, J. M., Complexation and Extraction of PAHs to the Aqueous Phase with a Dinuclear PtII Diazapyrenium-Based Metallacycle. *Chem. Eur. J.* **2010,** *16* (41), 12373-12380.

10.   Peinador, C.; Pia, E.; Blanco, V.; Garcia, M. D.; Quintela, J. M., Complexation of Pyrene in Aqueous Solution with a Self-Assembled Palladium Metallocycle. *Org. Lett.* **2010,** *12* (7), 1380-1383.

11.   Mal, P.; Breiner, B.; Rissanen, K.; Nitschke, J. R., White Phosphorus Is Air-Stable Within a Self-Assembled Tetrahedral Capsule. *Science* **2009,** *324* (5935), 1697-1699.

12.   Yamashina, M.; Sei, Y.; Akita, M.; Yoshizawa, M., Safe storage of radical initiators within a polyaromatic nanocapsule. *Nat. Commun.* **2014,** *5*, 4662-4668.

13.   Riddell, I. A.; Smulders, M. M. J.; Clegg, J. K.; Nitschke, J. R., Encapsulation, storage and controlled release of sulfur hexafluoride from a metal-organic capsule. *Chem. Commun.* **2011,** *47* (1), 457-459.

14.   Brown, C. J.; Toste, F. D.; Bergman, R. G.; Raymond, K. N., Supramolecular Catalysis in Metal-Ligand Cluster Hosts. *Chem. Rev.* **2015,** *115* (9), 3012-3035.

15.   Leenders, S. H. A. M.; Gramage-Doria, R.; de Bruin, B.; Reek, J. N. H., Transition metal catalysis in confined spaces. *Chem. Soc. Rev.* **2015,** *44* (2), 433-448.

16.   Lifschitz, A. M.; Rosen, M. S.; McGuirk, C. M.; Mirkin, C. A., Allosteric Supramolecular Coordination Constructs. *J. Am. Chem. Soc.* **2015,** *137* (23), 7252-7261.

17.   Wiester, M. J.; Ulmann, P. A.; Mirkin, C. A., Enzyme Mimics Based Upon Supramolecular Coordination Chemistry. *Angew. Chem., Int. Ed.* **2011,** *50* (1), 114-137.

18.   Hooley, R. J., No, Not That Way, the Other Way: Creating Active Sites in Self-Assembled Host Molecules. *Synlett* **2020,** *31* (15), 1448-1463.

19.   Lewis, J. E. M.; Gavey, E. L.; Cameron, S. A.; Crowley, J. D., Stimuli-responsive Pd_2L_4 metallosupramolecular cages: towards targeted cisplatin drug delivery. *Chem. Sci.* **2012,** *3*, 778-784.

20.   Preston, D.; Lewis, J. E. M.; Crowley, J. D., Multicavity $[Pd_nL_4]^{2n+}$ cages with controlled segregated binding of different guests. *J. Am. Chem. Soc.* **2017,** *139* (6), 2379-2386.

21.   Therrien, B.; Suess-Fink, G.; Govindaswamy, P.; Renfrew, A. K.; Dyson, P. J., The "complex-in-a-complex" cations $[(acac)_2M \subset Ru_6\text{-}(p\text{-}iPrC_6H_4Me)_6(tpt)_2(dhbq)_3]^{6+}$: a trojan horse for cancer cells. *Angew. Chem., Int. Ed.* **2008,** *47* (20), 3773-3776.

22.   Zheng, Y.-R.; Suntharalingam, K.; Johnstone, T. C.; Lippard, S. J., Encapsulation of Pt(IV) prodrugs within a Pt(II) cage for drug delivery. *Chem. Sci.* **2015,** *6* (2), 1189-1193.

23.   Murase, T.; Horiuchi, S.; Fujita, M., Naphthalene Diels-Alder in a Self-Assembled Molecular Flask. *J. Am. Chem. Soc.* **2010,** *132* (9), 2866-2867.

24.   Yoshizawa, M.; Fujita, M., Self-assembled coordination cage as a molecular flask. *Pure Appl. Chem.* **2005,** *77* (7), 1107-1112.

25.   Yoshizawa, M.; Fujita, M., Development of unique chemical phenomena within nanometer-sized, self-assembled coordination hosts. *Bull. Chem. Soc. Jpn.* **2010,** *83* (6), 609-618.

26.   Yoshizawa, M.; Klosterman, J. K.; Fujita, M., Functional Molecular Flasks: New Properties and Reactions within Discrete, Self-Assembled Hosts. *Angew. Chem., Int. Ed.* **2009,** *48* (19), 3418-3438.

27.   Therrien, B., Biologically relevant arene ruthenium metalla-assemblies. *CrystEngComm* **2015,** *17* (3), 484-491.

28.   Kaner, R. A.; Scott, P., Metallohelices: potential mimetics of α-helical peptides in cancer treatment. *Future Med. Chem.* **2015,** *7* (1), 1-4.

29.   Vasdev, R. A. S.; Preston, D.; Scottwell, S. O.; Brooks, H. J. L.; Crowley, J. D.; Schramm, M. P., Oxidatively locked $[Co_2L_3]^{6+}$ cylinders derived from bis(bidentate) 2-pyridyl-1,2,3-triazole "click" ligands: synthesis, stability, and antimicrobial studies. *Molecules* **2016,** *21* (11), 1548-1551.

30.   Bilbeisi, R. A.; Zarra, S.; Feltham, H. L. C.; Jameson, G. N. L.; Clegg, J. K.; Brooker, S.; Nitschke, J. R., Guest Binding Subtly Influences Spin Crossover (SCO) in an $Fe^{II}_4L_4$ Capsule. *Chem. - Eur. J.* **2013,** *19* (25), 8058-8062.

31.   Ferguson, A.; Squire, M. A.; Siretanu, D.; Mitcov, D.; Mathoniere, C.; Clerac, R.; Kruger, P. E., A face-capped $[Fe_4L_4]^{8+}$ spin crossover tetrahedral cage. *Chem. Commun.* **2013,** *49* (16), 1597-1599.

32.   Archer, R. J.; Hawes, C. S.; Jameson, G. N. L.; McKee, V.; Moubaraki, B.; Chilton, N. F.; Murray, K. S.; Schmitt, W.; Kruger, P. E., Partial spin crossover behaviour in a dinuclear iron(II) triple helicate. *Dalton Trans.* **2011,** *40* (45), 12368-12373.

33.   Frank, M.; Hey, J.; Balcioglu, I.; Chen, Y.-S.; Stalke, D.; Suenobu, T.; Fukuzumi, S.; Frauendorf, H.; Clever, G. H., Assembly and Stepwise Oxidation of Interpenetrated Coordination Cages Based on Phenothiazine. *Angew. Chem., Int. Ed.* **2013,** *52* (38), 10102-10106.

34.   Croué, V.; Goeb, S.; Sallé, M., Metal-driven self-assembly: the case of redox-active discrete architectures. *Chem. Commun.* **2015,** *51* (34), 7275-7289.

35.   Xu, L.; Wang, Y.-X.; Yang, H.-B., Recent advances in the construction of fluorescent metallocycles and metallocages via coordination-driven self-assembly. *Dalton Trans.* **2015,** *44* (3), 867-890.

36.   Chepelin, O.; Ujma, J.; Wu, X.; Slawin, A. M. Z.; Pitak, M. B.; Coles, S. J.; Michel, J.; Jones, A. C.; Barran, P. E.; Lusby, P. J., Luminescent, Enantiopure, Phenylatopyridine Iridium-Based Coordination Capsules. *J. Am. Chem. Soc.* **2012,** *134* (47), 19334-19337.

37.   Han, M.; Michel, R.; He, B.; Chen, Y.-S.; Stalke, D.; John, M.; Clever, G. H., Light-Triggered Guest Uptake and Release by a Photochromic Coordination Cage. *Angew. Chem., Int. Ed.* **2013,** *52* (4), 1319-1323.

38.   Hedstrom, L., Serine Protease Mechanism and Specificity. *Chem. Rev.* **2002,** *102* (12), 4501-4524.

39.   Weber, R. E.; Vinogradov, S. N., Nonvertebrate hemoglobins: functions and molecular adaptations. *Physiol. Rev.* **2001,** *81* (2), 569-628.

40.   May, K. L.; Yan, Q.; Tumer, N. E., Targeting ricin to the ribosome. *Toxicon* **2013,** *69*, 143-151.

41.   Lewis, J.; Crowley, J., Metallo-Supramolecular Self-Assembly with Reduced Symmetry Ligands. *ChemPlusChem* **2020,** *85* (5), 815-827.

42.   Sudan, S.; Li, R. J.; Jansze, S. M.; Platzek, A.; Rudolf, R.; Clever, G. H.; Fadaei-Tirani, F.; Scopelliti, R.; Severin, K., Identification of a Heteroleptic $Pd_6L_6L'_6$ Coordination Cage by Screening of a Virtual Combinatorial Library. *J. Am. Chem. Soc.* **2021,** *143* (4), 1773-1778.

43.   Tessarolo, J.; Lee, H.; Sakuda, E.; Umakoshi, K.; Clever, G. H., Integrative Assembly of Heteroleptic Tetrahedra Controlled by Backbone Steric Bulk. *J. Am. Chem. Soc.* **2021**, *143* (17), 6339–6344.

44.   Pullen, S.; Tessarolo, J.; Clever, G. H., Increasing structural and functional complexity in self-assembled coordination cages. *Chem. Sci.* **2021,** *12* (21), 7269-7293.

45.   Bardhan, D.; Chand, D. K., Palladium(II) Based Self-assembled Heteroleptic Coordination Architectures: A Growing Family. *Chem. Eur. J.* **2019,** *25*, 12241-12269.

46.   Debata, N. B.; Tripathy, D.; Chand, D. K., Self-assembled coordination complexes from various palladium(II) components and bidentate or polydentate ligands. *Coord. Chem. Rev.* **2012,** *256* (17–18), 1831-1945.

47.   McMorran, D. A.; Steel, P. J., The First Coordinatively Saturated, Quadruply Stranded Helicate and Its Encapsulation of a Hexafluorophosphate Anion. *Angew Chem., Int. Ed.* **1998,** *37*, 3295-3297.

48.   Saha, S.; Regeni, I.; Clever, G. H., Structure relationships between bis-monodentate ligands and coordination driven self-assemblies. *Coord. Chem. Rev.* **2018,** *374*, 1-14.

49.   Clever, G. H.; Punt, P., Cation-Anion Arrangement Patterns in Self-Assembled Pd_2L_4 and Pd_4L_8 Coordination Cages. *Acc. Chem. Res.* **2017,** *50* (9), 2233-2243.

50.   Han, M.; Engelhard, D. M.; Clever, G. H., Self-assembled coordination cages based on banana-shaped ligands. *Chem. Soc. Rev.* **2014,** *43* (6), 1848-60.

51.   Schmidt, A.; Casini, A.; Kühn, F. E., Self-assembled M_2L_4 coordination cages: Synthesis and potential applications. *Coord. Chem. Rev.* **2014**, *275* (0), 19-36.

52.   Jansze, S. M.; Wise, M. D.; Vologzhanina, A. V.; Scopelliti, R.; Severin, K., $Pd^{II}_2L_4$-type coordination cages up to three nanometers in size. *Chem. Sci.* **2017**, *8* (3), 1901-1908.

53.   August, D. P.; Nichol, G. S.; Lusby, P. J., Maximizing Coordination Capsule-Guest Polar Interactions in Apolar Solvents Reveals Significant Binding. *Angew Chem., Int. Ed.* **2016**, *55* (48), 15022-15026.

54.   Yamashina, M.; Tsutsui, T.; Sei, Y.; Akita, M.; Yoshizawa, M., A polyaromatic receptor with high androgen affinity. *Science Advances* **2019**, *5* (4), eaav3179.

55.   Tsutsui, T.; Kusaba, S.; Yamashina, M.; Akita, M.; Yoshizawa, M., Open versus Closed Polyaromatic Nanocavity: Enhanced Host Abilities toward Large Dyes and Pigments. *Chem. Eur. J.* **2019**, *25* (17), 4320-4324.

56.   Yamashina, M.; Akita, M.; Hasegawa, T.; Hayashi, S.; Yoshizawa, M., A polyaromatic nanocapsule as a sucrose receptor in water. *Science Advances* **2017**, *3* (8) e170112.

57.   Kishi, N.; Li, Z.; Sei, Y.; Akita, M.; Yoza, K.; Siegel, J. S.; Yoshizawa, M., Wide-Ranging Host Capability of a Pd^{II}-Linked M_2L_4 Molecular Capsule with an Anthracene Shell. *Chem. Eur. J.* **2013**, *19* (20), 6313-6320.

58.   Li, Z.; Kishi, N.; Yoza, K.; Akita, M.; Yoshizawa, M., Isostructural M_2L_4 Molecular Capsules with Anthracene Shells: Synthesis, Crystal Structures, and Fluorescent Properties. *Chem. Eur. J.* **2012**, *18* (27), 8358-8365.

59.   Kishi, N.; Li, Z.; Yoza, K.; Akita, M.; Yoshizawa, M., An M_2L_4 Molecular Capsule with an Anthracene Shell: Encapsulation of Large Guests up to 1 nm. *J. Am. Chem. Soc.* **2011**, *133* (30), 11438-11441.

60.   Chen, B.; Horiuchi, S.; Holstein, J. J.; Tessarolo, J.; Clever, G. H., Tunable Fullerene Affinity of Cages, Bowls and Rings Assembled by Pd(II) Coordination Sphere Engineering. *Chem. Eur. J.* **2019**, *25* (65), 14921-14927.

61.   Lewis, J. E. M.; Gavey, E. L.; Cameron, S. A.; Crowley, J. D., Stimuli-responsive Pd_2L_4 metallosupramolecular cages: towards targeted cisplatin drug delivery. *Chem. Sci.* **2012**, *3* (3), 778-784.

62.   Lewis, J. E. M.; Elliott, A. B. S.; McAdam, C. J.; Gordon, K. C.; Crowley, J. D., 'Click' to functionalise: synthesis, characterisation and enhancement of the physical properties of a series of exo- and endo-functionalised Pd_2L_4 nanocages. *Chem. Sci.* **2014**, *5* (5), 1833-1843.

63.   Preston, D.; White, K. F.; Lewis, J. E. M.; Vasdev, R. A. S.; Abrahams, B. F.; Crowley, J. D., Solid-State Gas Adsorption Studies with Discrete Palladium(II) $[Pd_2(L)_4]^{4+}$ Cages. *Chem. Eur. J.* **2017**, *23* (44), 10559-10567.

64.   Johnstone, M. D.; Schwarze, E. K.; Ahrens, J.; Schwarzer, D.; Holstein, J. J.; Dittrich, B.; Pfeffer, F. M.; Clever, G. H., Desymmetrization of an Octahedral Coordination Complex Inside a Self-Assembled Exoskeleton. *Chem. Eur. J.* **2016**, *22* (31), 10791-10795.

65.   Clever, G. H.; Kawamura, W.; Tashiro, S.; Shiro, M.; Shionoya, M., Stacked Platinum Complexes of the Magnus' Salt Type Inside a Coordination Cage. *Angew. Chem., Int. Ed.* **2012**, *51* (11), 2606-2609.

66.   Lewis, J. E. M.; Crowley, J. D., Exo- and endo-hedral interactions of counteranions with tetracationic Pd_2L_4 metallosupramolecular architectures. *Supramol. Chem.* **2014**, *26* (3-4), 173-181.

67.   Steel, P. J.; McMorran, D. A., Selective Anion Recognition by a Dynamic Quadruple Helicate. *Chem. Asian J.* **2019,** *14* (8), 1098-1101.

68.   Zhou, L.-P.; Sun, Q.-F., A self-assembled Pd_2L_4 cage that selectively encapsulates nitrate. *Chem. Commun.* **2015,** *51* (94), 16767-16770.

69.   Chand, D. K.; Biradha, K.; Fujita, M., Self-assembly of a novel macrotricyclic Pd(II) metallocage encapsulating a nitrate ion. *Chem. Commun.* **2001,** (17), 1652-1653.

70.   Preston, D.; Fox-Charles, A.; Lo, W. K. C.; Crowley, J. D., Chloride triggered reversible switching from a metallosupramolecular $[Pd_2L_4]^{4+}$ cage to a $[Pd_2L_2Cl_4]$ metallo-macrocycle with release of endo- and exo-hedrally bound guests. *Chem. Commun.* **2015,** *51* (43), 9042-9045.

71.   Vasdev, R. A. S.; Findlay, J. A.; Garden, A. L.; Crowley, J. D., Redox active $[Pd_2L_4]^{4+}$ cages constructed from rotationally flexible 1,1′-disubstituted ferrocene ligands. *Chem. Commun.* **2019,** *55*, 7506-7509.

72.   Clever, G. H.; Kawamura, W.; Shionoya, M., Encapsulation versus Aggregation of Metal-Organic Cages Controlled by Guest Size Variation. *Inorg. Chem.* **2011,** *50* (11), 4689-4691.

73.   Clever, G. H.; Tashiro, S.; Shionoya, M., Light-Triggered Crystallization of a Molecular Host-Guest Complex. *J. Am. Chem. Soc.* **2010,** *132* (29), 9973-9975.

74.   Clever, G. H.; Shionoya, M., A pH Switchable Pseudorotaxane Based on a Metal Cage and a Bis-anionic Thread. *Chem. Eur. J.* **2010,** *16* (39), 11792-11796.

75.   Clever, G. H.; Tashiro, S.; Shionoya, M., Inclusion of Anionic Guests inside a Molecular Cage with Palladium(II) Centers as Electrostatic Anchors. *Angew. Chem., Int. Ed.* **2009,** *48* (38), 7010-7012.

76.   Pöthig, A.; Casini, A., Recent Developments of Supramolecular Metal-based Structures for Applications in Cancer Therapy and Imaging. *Theranostics* **2019,** *9* (11), 3150-3169.

77.   Spicer, R. L.; Stergiou, A. D.; Young, T. A.; Duarte, F.; Symes, M. D.; Lusby, P. J., Host-Guest-Induced Electron Transfer Triggers Radical-Cation Catalysis. *J. Am. Chem. Soc.* **2020,** *142* (5), 2134-2139.

78.   Martí-Centelles, V.; Spicer, R.; Lusby, P., Non-Covalent Allosteric Regulation of Capsule Catalysis. *Chem. Sci.* **2020,** *11* (12), 3236-3240.

79.   Young, T. A.; Marti-Centelles, V.; Wang, J.; Lusby, P. J.; Duarte, F., Rationalizing the Activity of an "Artificial Diels-Alderase": Establishing Efficient and Accurate Protocols for Calculating Supramolecular Catalysis. *J. Am. Chem. Soc.* **2020,** *142* (3), 1300-1310.

80.   Marti-Centelles, V.; Lawrence, A. L.; Lusby, P. J., High Activity and Efficient Turnover by a Simple, Self-Assembled "Artificial Diels-Alderase". *J. Am. Chem. Soc.* **2018,** *140* (8), 2862-2868.

81.   Bloch, W. M.; Clever, G. H., Integrative self-sorting of coordination cages based on 'naked' metal ions. *Chem. Commun.* **2017,** *53* (61), 8506-8516.

82.   Holloway, L. R.; Bogie, P. M.; Hooley, R. J., Controlled self-sorting in self-assembled cage complexes. *Dalton Trans.* **2017,** *46* (43), 14719-14723.

83.   Tsutsui, T.; Catti, L.; Yoza, K.; Yoshizawa, M., An atropisomeric M_2L_4 cage mixture displaying guest-induced convergence and strong guest emission in water. *Chem. Sci.* **2020,** *11* (31), 8145-8150.

84.   Lisboa, L. S.; Findlay, J. A.; Wright, L. J.; Hartinger, C. G.; Crowley, J. D., A Reduced-Symmetry Heterobimetallic [PdPtL$_4$]$^{4+}$ Cage: Assembly, Guest Binding, and Stimulus-Induced Switching. *Angew. Chem., Int. Ed.* **2020,** *59* (27), 11101 –11107.

85.   Bloch, W. M.; Abe, Y.; Holstein, J. J.; Wandtke, C. M.; Dittrich, B.; Clever, G. H., Geometric Complementarity in Assembly and Guest Recognition of a Bent Heteroleptic cis-[Pd$_2$L$_{A2}$L$_{B2}$] Coordination Cage. *J. Am. Chem. Soc.* **2016,** *138* (41), 13750-13755.

86.   Zhu, R.; Bloch, W. M.; Holstein, J. J.; Mandal, S.; Schäfer, L. V.; Clever, G. H., Donor-Site-Directed Rational Assembly of Heteroleptic cis-[Pd$_2$L$_2$L′$_2$] Coordination Cages from Picolyl Ligands. *Chem. Eur. J.* **2018,** *24* (49), 12976-12982.

87.   Bloch, W. M.; Holstein, J. J.; Hiller, W.; Clever, G. H., Morphological Control of Heteroleptic cis- and trans-Pd$_2$L$_2$L′$_2$ Cages. *Angew. Chem., Int. Ed.* **2017,** *56* (28), 8285-8289.

88.   Johnson, A. M.; Hooley, R. J., Steric Effects Control Self-Sorting in Self-Assembled Clusters. *Inorg. Chem.* **2011,** *50* (11), 4671-4673.

89.   Chen, B.; Holstein, J. J.; Platzek, A.; Schneider, L.; Wu, K.; Clever, G. H., Cooperativity of steric bulk and H-bonding in coordination sphere engineering: heteroleptic Pd^{II} cages and bowls by design. *Chem. Sci.* **2022,** *13* (6), 1829-1834.

90.   Li, R. J.; Fadaei-Tirani, F.; Scopelliti, R.; Severin, K., Tuning the Size and Geometry of Heteroleptic Coordination Cages by Varying the Ligand Bent Angle. *Chem. Eur. J.* **2021,** *27* (36), 9439-9445.

91.   Findlay, J. A.; Patil, K. M.; Gardiner, M. G.; MacDermott-Opeskin, H. I.; O'Mara, M. L.; Kruger, P. E.; Preston, D., Heteroleptic Tripalladium(II) Cages. *Chem. Asian J.* **2022,** e202200093.

92.   Yamashina, M.; Yuki, T.; Sei, Y.; Akita, M.; Yoshizawa, M., Anisotropic Expansion of an M2L4 Coordination Capsule: Host Capability and Frame Rearrangement. *Chem. Eur. J.* **2015,** *21* (11), 4200-4204.

93.   Preston, D.; Barnsley, J. E.; Gordon, K. C.; Crowley, J. D., Controlled Formation of Heteroleptic [Pd$_2$(L$_a$)$_2$(L$_b$)$_2$]$^{4+}$ Cages. *J. Am. Chem. Soc.* **2016,** *138* (33), 10578-85.

94.   **Others have developed related 2 picolyl ligands, these do not behave in the same way as the 2-amino substituted system, confirming the importance of the hydrogen bonding. The 2 picolyl ligands (L$_{pc}$) can be used to generate heteroleptic cis-[Pd$_2$(L$_{pc}$)$_2$(L$_{pc}$′)$_2$] when combined with isomeric 6 picolyl ligands (L$_{pc}$′), see reference 86.**

95.   Tripathy, D.; Debata, N. B.; Naik, K. C.; Sahoo, H. S., Coordination driven discrete metallopolygons and cages from unsymmetric bidentate ligands. *Coord. Chem. Rev.* **2022,** *456*, 214396.

96.   Lewis, J. E. M.; Tarzia, A.; White, A. J. P.; Jelfs, K. E., Conformational control of Pd$_2$L$_4$ assemblies with unsymmetrical ligands. *Chem. Sci.* **2020,** *11* (3), 677-683.

97.   Tarzia, A.; Lewis, J. E. M.; Jelfs, K. E., High-Throughput Computational Evaluation of Low Symmetry Pd$_2$L$_4$ Cages to Aid in System Design**. *Angew. Chem., Int. Ed.* **2021,** *60* (38), 20879-20887.

98.   Yu, H.; Li, J.; Shan, C.; Lu, T.; Jiang, X.; Shi, J.; Wojtas, L.; Zhang, H.; Wang, M., Conformational Control of a Metallo-Supramolecular Cage via the Dissymmetrical Modulation of Ligands. *Angew. Chem., Int. Ed.* **2021,** *60* (51), 26523-26527.

99.   Li, R.-J.; Marcus, A.; Fadaei-Tirani, F.; Severin, K., Orientational self-sorting: formation of structurally defined Pd_4L_8 and Pd_6L_{12} cages from low-symmetry dipyridyl ligands. *Chem. Commun.* **2021,** *57* (78), 10023-10026.

100.   Ogata, D.; Yuasa, J., Dynamic Open Coordination Cage from Nonsymmetrical Imidazole–Pyridine Ditopic Ligands for Turn-On/Off Anion Binding. *Angew. Chem., Int. Ed.* **2019,** *58*,18424–18428.

101.   Mishra, S. S.; Kompella, S. V. K.; Krishnaswamy, S.; Balasubramanian, S.; Chand, D. K., Low-Symmetry Self-Assembled Coordination Complexes with Exclusive Diastereoselectivity: Experimental and Computational Studies. *Inorg. Chem.* **2020,** *59* (17), 12884-12894.

102.   Lewis, J. E. M., Multi-functional, Low Symmetry Pd_2L_4 Nanocage Libraries*. *Chem. Eur. J.* **2021,** *27* (13), 4454-4460.

103.   Sen, S. K.; Natarajan, R., Influence of Conformational Change and Interligand Hydrogen Bonding in a Chiral Metal–Organic Cage. *Inorg. Chem.* **2019,** *58* (11), 7180-7188.

104.   Yue, N. L. S.; Eisler, D. J.; Jennings, M. C.; Puddephatt, R. J., Macrocyclic and Lantern Complexes of Palladium(II) with Bis(amidopyridine) Ligands: Synthesis, Structure, and Host−Guest Chemistry. *Inorg. Chem.* **2004,** *43* (24), 7671-7681.

105.   Yue, N.; Qin, Z.; Jennings, M. C.; Eisler, D. J.; Puddephatt, R. J., Host complexes that adapt to their guests: amphitopic receptors. *Inorg. Chem. Commun.* **2003,** *6* (9), 1269-1271.

106.   Dasary, H.; Jagan, R.; Chand, D. K., Ligand Isomerism in Coordination Cages. *Inorg. Chem.* **2018,** *57* (19), 12222-12231.

107.   Vasdev, R. A. S.; Gaudin, L. F.; Preston, D.; Jogy, J. P.; Giles, G. I.; Crowley, J. D., Anticancer Activity and Cisplatin Binding Ability of Bis-Quinoline and Bis-Isoquinoline Derived $[Pd_2L_4]^{4+}$ Metallosupramolecular Cages. *Front. Chem.* **2018,** *6* (563), 1-9.

108.   Preston, D.; McNeill, S. M.; Lewis, J. E. M.; Giles, G. I.; Crowley, J. D., Enhanced kinetic stability of $[Pd_2L_4]^{4+}$ cages through ligand substitution. *Dalton Trans.* **2016,** *45* (19), 8050-60.

109.   Northrop, B. H.; Yang, H.-B.; Stang, P. J., Second-Order Self-Organization in Coordination-Driven Self-Assembly: Exploring the Limits of Self-Selection. *Inorg. Chem.* **2008,** *47* (23), 11257-11268.

110.   **Stang and co-workers have experimented with polyethylene glycol- and alkyl-substituted dipyridyl ligands and Pt(II) molecular "clips" in an attempted to generate self-sorted metallomacrocycles. When the components are combined in a 2:1:1 metal:ligand:ligand ratio in CD_3COCD_3/D_2O and heated at 55°C for 18 hours, a variety of products are observed depending on the chain length. When the shortest chains were used (C6/DEG) the target heteroleptic amphiphilic molecule was the dominant species, as confirmed through ^{31}P NMR spectroscopy and mass spectrometry, but the two homomeric rectangles are also present in equal ratio with each other. In contrast to this, when longer chain were used (C18/HEG = hexaethylene glycol), the opposite is observed: narcissistic self-organisation is dominant and the homomeric compounds are the main species in the ^{31}P NMR and mass spectra, with small amounts of the target heteroleptic complex present as well. The authors have hypothesised that this is due to the long chained ligands aggregating together in hydrophobic and hydrophilic assemblies in solution before they react with the Pt(II)**

molecular clip, thus reducing the likelihood of forming heteroleptic complexes. See reference 109.

111.   Johnson, A. M.; Moshe, O.; Gamboa, A. S.; Langloss, B. W.; Limtiaco, J. F. K.; Larive, C. K.; Hooley, R. J., Synthesis and Properties of Metal-Ligand Complexes with Endohedral Amine Functionality. *Inorg. Chem.* **2011,** *50* (19), 9430-9442.

112.   Liao, P.; Langloss, B. W.; Johnson, A. M.; Knudsen, E. R.; Tham, F. S.; Julian, R. R.; Hooley, R. J., Two-component control of guest binding in a self-assembled cage molecule. *Chem. Commun.* **2010,** *46* (27), 4932-4934.

113.   Kim, T. Y.; Lucas, N. T.; Crowley, J. D., A diaryl-linked $[Pd_2L_4]^{4+}$ metallosupramolecular architecture: synthesis, structures and cisplatin binding studies. *Supramol. Chem.* **2015,** *27* (11-12), 734-745.

114.   Walker, S. E.; Boer, S. A.; Malcomson, T.; Paterson, M. J.; Tuck, K. L.; Turner, D. R., Steric control of sorting regimes in self-assembled cages. *Chem. Commun.* **2021,** *57* (93), 12456-12459.

115.   Neese, F., The ORCA program system. *Wiley Interdiscip. Rev.: Comput. Mol. Sci.* **2012,** *2* (1), 73-78.

116.   **The 2A-tripy and 3A-tripy ligands from reference 93 behave differently. When $[Pd_2(tripy)_4]^{4+}$ was treated with 3A-tripy $[Pd_2(3A-tripy)_4]^{4+}$ was obtained quantitatively. Conversely, when $[Pd_2(tripy)_4]^{4+}$ was treated with 2A-tripy the heteroleptic cis-$[Pd(2A-tripy)_2(tripy)_2]^{4+}$ complex formed, suggesting that a combination of hydrogen bonding and steric effects were required to generate the mixed ligand system.**

117.   Jeffrey, G. A., *An Introduction to Hydrogen Bonding.* Oxford University Press: New York, 1997.

118.   Johnson, E. R.; Keinan, S.; Mori-Sánchez, P.; Contreras-García, J.; Cohen, A. J.; Yang, W., Revealing Noncovalent Interactions. *J. Am. Chem. Soc.* **2010,** *132* (18), 6498-6506.

119.   **While the majority of metallosupramolecular architectures are assembled under thermodynamic control this is not always the the case. There have been several systems reported where the assembly is kinetically controlled, see references 120-124 for examples**.

120.   Takahashi, S.; Tateishi, T.; Sasaki, Y.; Sato, H.; Hiraoka, S., Towards kinetic control of coordination self-assembly: a case study of a Pd_3L_6 double-walled triangle to predict the outcomes by a reaction network model. *Phys. Chem. Chem. Phys.* **2020,** *22* (45), 26614-26626.

121.   Nakagawa, M.; Kai, S.; Kojima, T.; Hiraoka, S., Energy-Landscape-Independent Kinetic Trap of an Incomplete Cage in the Self-Assembly of a Pd_2L_4 Cage. *Chem. - Eur. J.* **2018,** *24* (35), 8804-8808.

122.   Hiraoka, S.; Takahashi, S.; Sato, H., Coordination Self-assembly Processes Revealed by Collaboration of Experiment and Theory: Toward Kinetic Control of Molecular Self-assembly. *Chem. Rec.* **2021**, 21, 443– 459.

123.   Tateishi, T.; Takahashi, S.; Okazawa, A.; Marti-Centelles, V.; Wang, J.; Kojima, T.; Lusby, P. J.; Sato, H.; Hiraoka, S., Navigated Self-Assembly of a Pd_2L_4 Cage by Modulation of an Energy Landscape under Kinetic Control. *J. Am. Chem. Soc.* **2019,** *141* (50), 19669-19676.

124.   Foianesi-Takeshige, L. H.; Takahashi, S.; Tateishi, T.; Sekine, R.; Okazawa, A.; Zhu, W.; Kojima, T.; Harano, K.; Nakamura, E.; Sato, H.; Hiraoka, S., Bifurcation of self-assembly pathways to sheet or cage controlled by kinetic template effect. *Commun. Chem.* **2019,** *2* (1), 128.

TOC
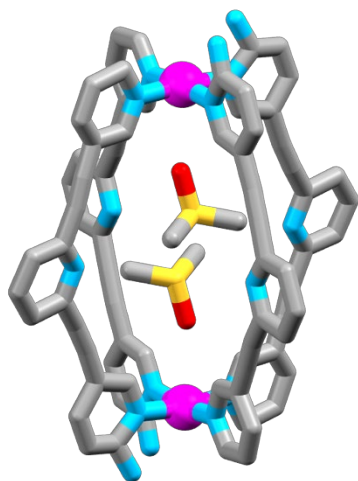
Efforts to use supramolecular (dispersion and hydrogen bonding) forces and solvophobic effects to generate isomerically pure $[Pd_2(L)_4]^{4+}$ cage architectures from a family of new reduced symmetry ditopic tripyridyl ligands are reported. Dispersion forces and solvophobic effects provided no isomer selectivity. However, the combination of hydrogen bonding interactions and steric effects enabled the quantative formation of the *cis*-HHTT cage architecture.